18th WORLD CONFERENCE ON EARTHQUAKE ENGINEERING
WCEE2024
MILAN

MILAN, ITALY
30th JUNE - 5th JULY 2024
www.wcee2024.it

HEURISTIC-BASED SEQUENTIAL DECISION-MAKING ON POST-SHOCK EMERGENCY RESPONSE OF MODERN ROAD NETWORKS

L. Sun[1], S. Yang[2], X. Liu[3]

[1]Cardiff University, Cardiff, United Kingdom, sunl32@cardiff.ac.uk

[2]Dalian University of Technology, Dalian, China

[3]University College London, London, United Kingdom

Abstract: Modern Road Networks (RNs) have shown to be susceptible to functionality losses, due to the damage of their critical components (*e.g.*, bridges), under hazard events. Besides, the functionality losses of those RNs would often have a knock-on effect on the resilience of the whole urban community, which they serve. Against this backdrop, the post-hazard emergency response has recently emerged as a promising pathway towards the future, hazard-resilient infrastructure systems, including RNs. However, under real-world hazard events, it would be rather challenging to plan those emergency response campaigns that are often executed by an array of independent repair groups. To address this challenge, a multi-agent-based model (MABM) is established in this study, on the emergency response of hazard-impacted RNs. In this MABM, each repair group is modelled as an autonomous agent, whose decision-making is driven by different heuristic-based strategies. To demonstrate its applicability, such a MABM is applied to a real-world RN under catastrophic earthquake scenarios, and the impact of different heuristics on the performance of the emergency response campaign has been exmained and elucidated.

1 Introduction

The well-being of modern urban communities is underpinned by a whole host of Critical Infrastructure Systems (CISs) that have been cybernetically engineered and networked, to ensure an enduring functionality supply (Kröger and Zio 2011). Meanwhile, due to those ever-growing intra- and interdependences, insignificant damage or dysfunction incurred by any single CIS could propagate, and thus trigger a potentially full-blown cascading failure of the whole system of networked CISs (Buldyrev et al. 2010, Brummitt et al. 2012, Bashan et al. 2013, Zhao and Sun 2021). The inherent vulnerability of those CISs will decay the resilience of modern urban communities (Helbing 2013), as demonstrated by real-world catastrophes, *e.g.*, natural hazards. In particular, the earthquake-induced death toll and property losses have often found to be unmatched by those associated with other natural hazards, for many of the urban communities across the spectrum of wealth (Nichols and Rodgers 2017). The observation on real-world earthquake hazards have further indicated that, one of the root causes for the lack of seismic resilience lies in the inability of state-of-the-art disaster management systems of those communities to deliver an expeditious and effective recovery in the immediate aftermath of earthquakes (IAoEs). As a result, the earthquake-initiated losses could often be significantly exacerbated (Young et al. 2004, Funabashi and Kitazawa 2012), while the corresponding death toll can be also rising sharply thereafter (Zhang et al. 2012, Zhao et al. 2023). Against this backdrop, the post-shock emergency response (ER) that aims at minimizing the functionality losses of CISs throughout IAoEs, and ultimately, mitigating the potential exacerbation of the earthquake-initiated damage of those physical systems has emerged as a new and promising pathway towards resilient CISs in the future (Sun et al. 2021).

Nevertheless, it is also noteworthy that, it could be very challenging to plan and discover the “optimal” sequence of those ER campaigns following exhaustive search-based optimization routines (Ausiello et al. 2003, Bocchini and Frangopol 2012), in light of the immensity of the state space of real-world CISs under damaging earthquakes. To address such a challenge, Sun et al. (2022) have leveraged the latest advancement in the domain of deep reinforcement learning to establish an autonomous planning system of the post-shock ER of CISs. Without losses of generality, they have been focusing on the modern Road Networks (RNs), which often play a strategically vital role with respect to the resilience of the whole hazard-impacted urban community. Accordingly, the rapid repair of those earthquake-collapsed bridges, which usually turned to be the weakest link of modern RNs under damaging earthquakes (Kilanitis and Sextos 2019) have been adopted as a viable approach to the post-shock ER of those infrastructure assets. By restoring the functionality of those collapsed bridges to a fractional, yet minimal acceptable level, the ER would enable the transfer of the wounded and the restoration of many other CISs. Such a newly-established autonomous planning system has been applied to the RN in Luchon city, France, under hypothetical scenarios of catastrophic earthquakes. The simulation outcome has highlighted that, this machine learning-driven planning system has been able to chart a pathway to fulfil the optimization goal of the ER campaign, by balancing the trade-off between the repairability and criticality of collapsed bridges.

Despite the progress, it shall also be highlighted that, it is often computationally expensive to generate huge amount of the training data to enable that autonomous planning system, especially, when it comes to the large-scale, interwoven CISs. Furthermore, that planning system is often uninterpretable to engineers and stakeholders, which would further limit its applicability. Against this backdrop, by drawing useful experiences from the success of that system, a scalable heuristic on the sequential decision-making on the post-shock ER of RNs has been proposed in this paper. Accordingly, a multi agent-based model (MABM) is established in this paper, where the two squads in charge of the ER of collapsed bridges and the full repair of those moderately-damaged ones, respectively, have been included. This MABM has then been employed to model the ER campaign of the same RN that has already been discussed above, under different seismic scenarios. In particular, the difference between the behaviour of the ER campaigns guided by the newly-proposed heuristic and the other, established ones have been investigated and highlighted.

2 The modelling framework

In this paper, resilience of earthquake-impacted RNs is examined in the separated Absorption and IAoE stages, in the time domain (Ouyang et al. 2012, Sun et al. 2021). Specifically, the focus of the Absorption stage is the assessment on the functionality loss of RNs under the shock, as a result of the earthquake-initiated damage of a host of their components. It is noteworthy that, only the damage of bridge structures is considered in this study, whereas those road segments connecting them are assumed to be intact (Kilanitis and Sextos 2019). Throughout the ensuing IAoE, the MABM established in this paper will be employed to track the functionality of earthquake-impacted RNs that is collectively shaped by the ER and the concurrent full repair campaigns. In particular, in light of the long-lasting bottleneck effect of collapsed bridges (Lin et al. 2010, Radio New Zealand 2011) throughout IAoEs, the post-shock ER has been characterized as the endeavour to restore the functionality of those bridges to a minimal yet acceptable level, whereby the emergency rescue and restoration can be undertaken. In parallel, the full repair campaign aims at a full restoration of the functionality of those moderately-damaged bridges.

2.1 Vulnerability analysis at Absorption stages

At this stage, the remaining functionality of each of the bridge associated with the RN of interest will be examined, given the intensity measure of the earthquake ground motion at its geographic site obtained from seismic attenuation models (Mackie and Stojadinovic 2006). However, under real-world seismic hazards, the relationship between seismic damage and the corresponding functionality loss of bridge structures is inherently case-specific and thus challenging to quantify (Gehl and D’Ayala 2016, Gehl and D’Ayala 2018). To address this challenge, seismic fragility functions are employed in this study to determine the Damage State (DS) of bridge structures under seismic hazards, at first. Accordingly, a total of three DSs, *i.e.*, no damage (DS1), moderate damage (DS2), and collapse (DS3), respectively, are considered. The vulnerability of those damaged bridges is then assessed by quantifying their remaining functionality, pursuant to their DSs. To that end, the bridge functionality loss metrics proposed by Gehl and D'Ayala (2018) is employed in this paper. Quantitatively, it is therefore assumed that those bridges with DS3 are closed to any vehicular traffic, while those ones with DS2 are set to remain passable, but the travelling speed will be reduced to 25% of the pre-shock level.

2.2 Functionality restoration throughout IAoEs

In this study, the functionality of the earthquake-damaged RNs is assumed to start to be restored, since the beginning of IAoEs, as illustrated in Fig. 1. As mentioned above, the dynamic of such a restoration would be collectively shaped by the ER and the corresponding full repair campaigns. It shall also be particularly highlighted that, a looped interdependence between those two campaigns, run by different stakeholders, would often emerge under real-world seismic hazards (Sun et al. 2021). As an endeavour to account for the significant impact of that interdependence on the post-shock ER campaigns, a multi agent-based model (MABM) is proposed in this study, as an adaptive approach to the simulation on the dynamic interplay among intelligent entities (Sun 2017). Without losses of generality, in this study, both the ER and the full repair are supposed to be executed by one repair squad only. Accordingly, in the MABM, the behaviour of those two squads will be modelled by two separate agents, denoted as the Agent a and Agent b, respectively, as shown in Fig. 1. Meanwhile, the behaviour of both those two agents throughout ER campaigns will be shaped by a set of pre-defined behavioural attributes, in each realization of the simulation.

Under real-world seismic catastrophes, the time span regarding the repair (either the full or partial ones) of each individual bridge will be dependent upon the severity of the damage, the accessibility and the structural characteristic of the bridge, as well as the resourcefulness of the repair squads, etc. As a viable approach to consider those impacts, regarding any collapsed bridge j ($j = 1, 2, \ldots, N$, where N refers to the total number of bridges collapsed), the time needed (denoted as RT_j) to complete the partial repair, *i.e.*, the ER will be quantified following the Eq. (1):

$$RT_{,j} = TT_j + \frac{F_j}{E_{er} * \omega^{n(j)}} * \frac{\text{Span(j)}}{50}, \qquad \text{if } Span\ (j) \leq 50\text{m or}$$

$$RT_{,j} = TT_j + \frac{F_j}{E_{er} * \omega^{n(j)}} * \left(\frac{\text{Span(j)}}{50}\right)^2, \qquad \text{if } Span\ (j) > 50\text{m}, \tag{1}$$

with $j = 1: N_r$, and

$$TT_1 = SD_0 / V_{er} \tag{2}$$

$$TT_j = SD_j / V_{er}, \text{ for } j = 2: N_r \tag{3}$$

where TT_1 is the time required to reach the first bridge, since the earthquake event. Pursuant to the topology of the RN, this travel time between the ER centre and this bridge is determined by the length of the shortest path between the two sites (denoted as SD_0), and V_{er} that is the travel velocity of Agent a. Accordingly, RT_1 can be obtained by TT_1 plus the repair time, as shown in Eq. (1). It is noteworthy that, in this equation, F_j denotes the targeted functionality level that is to be restored by Agent a. In this study, such a level is set to be the restored accessibility of the bridge, but with the allowable travelling speed reduced to 50% of the pre-shock level. Meanwhile, E_{er} refers to the expected repair efficiency of Agent a. However, in this paper, this parameter is reduced by a factor of ω^n (ω<1), to account for the impact of the full repair campaign on the ER. Accordingly, n(j) denotes the number of damaged bridges (with either DS2, or DS3) associated with the shortest path between the last bridge where ER has been completed and the one Agent a is heading to tackle. Hence, such a parameter will assume a new value for each ER loop, based on the number and location of bridges repaired, as shown in Fig.1. Furthermore, regarding each individual bridge j, the time required to complete the ER is set to increase linearly with its span (denoted as Span (j)), if shorter than 50m. By comparison, such a time will increase quadratically with Span (j), if larger than 50m (Yeh et al. 2015, Sun et al. 2021). The simulation will be run following Eqs. (1-3), in an iterative way, until the ER of all the collapsed bridges have been finalized.

In parallel, the full repair campaign run by Agent b will be tracked in a similar way, yet with different behaviour attributes that are denoted as V_{fr} and E_{fr}, respectively. Like Agent a, V_{fr} and E_{fr} refer to the travel velocity and the repair efficiency of Agent b, respectively. However, it shall be highlighted that Agent B would likely encounter inaccessible paths, due to the presence of bridges with DS3. Regarding such cases, before being able to reach a particular bridge scheduled for the full repair, Agent b is assumed to be waiting until the restoration (enabled by Agent a) of the accessibility of those collapsed bridges occluding its available pathway forward. By doing so, the behaviour of ER on the full repair campaign, and ultimately, the dynamic interplay between the two agents has been thereby taken into account.

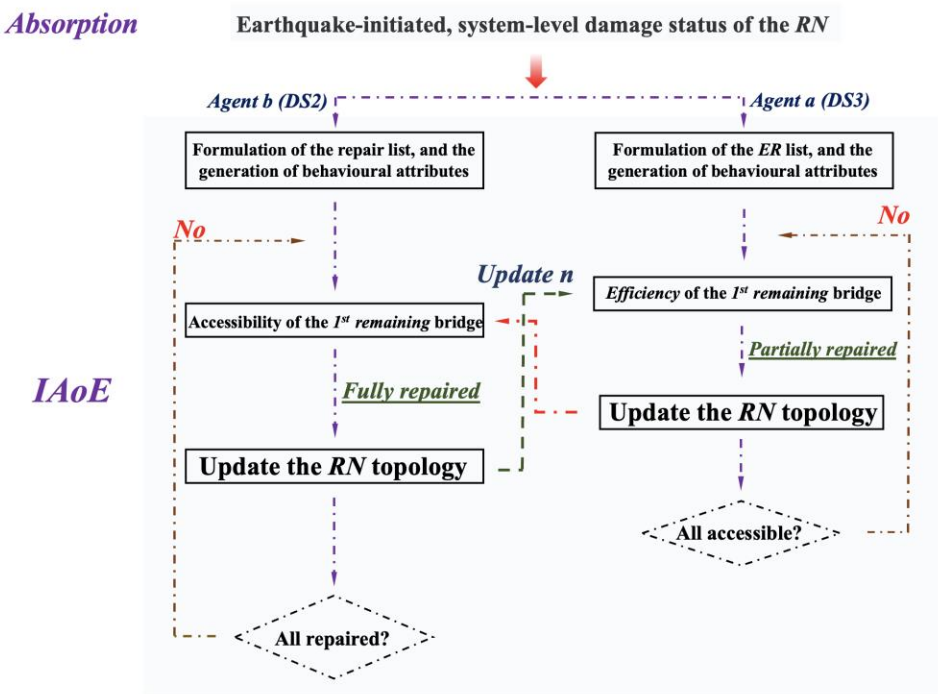

Figure 1. Post-shock emergency response campaign modelled following the MABS.

2.3 The optimization objective of ER campaigns

In this study, the gross weighted loss (GWL) is chosen as an inclusive optimization goal of the post-shock ER of RNs (Sun et al. 2022). Mathematically, regarding each of the realization of the campaign, GWL is computed following the Eq. (4):

$$GWL = \sum_{t=0}^{T_f} \sum_{k=1}^{N_b} B_k \times RS_{k,t} \tag{4}$$

Here, T_f refers to the time point when the whole ER campaign has been finalized. Meanwhile, B_k and $RS_{k,t}$ refer to the betweenness value of the bridge k (k=1, 2,…,N_b, where N_b is the total number of bridges of the RN), and the recovery state of this bridge at time point t, respectively. For each individual bridge, its recovery state can be 0, 0.5, 1, and 3, indicating the total recovery (or intact under the seismic hazard), partial repair, moderate damage, and collapse, respectively.

It is noteworthy that, from the standpoint of graph theory, the betweenness is one of the most definitive measures on the criticality of each single node, regarding the connectivity of the whole network (Brandes 2001). Quantitatively, the betweenness centrality of bridge k, denoted as B(k), will be computed following Eq. (5), in this paper:

$$B(k) = \frac{\sum_{s \neq k \neq t} \sigma_{st}(k)}{\sigma_{tot}} \tag{5}$$

Here, σ_{tot} denotes the total number of shortest paths associated with the whole RN of interest, while $\sigma_{st}(k)$ assume a value of *1*, when the shortest path goes through k, and *0* otherwise.

2.4 Sequential decision-making on the post-shock ER campaigns

Given the interdependence between the ER and the corresponding full repair, it is vital to plan, *i.e.*, find out the "optimal" sequence of those two campaigns to fulfil the optimization objective, namely, the GWL. It shall be noted that, it would be often challenging to discover those sequences, given the enormous state space of modern CISs, *e.g.*, RNs. It will be thus unviable to resort to brute-force search-based optimization routines, with respect to real-world catastrophes (Powell 2019). Against this backdrop, based on engineering reasoning, a host of different heuristic-based strategies have been considered and employed to plan the ER campaigns of earthquake-impacted RNs. To that end, a span-based strategy has been proposed by Sun et al (2021), at first. Following such a strategy, all the collapsed bridges will be sequenced (in the ascending order) based on their span, which serves as a measure on the ease of the partial repair of each individual bridge. In parallel, given the proportional sensitivity of GWL to the criticality of individual bridges (as highlighted in Eq. (4)), justifiably, a betweenness-based strategy that sequences all those bridges based on their betweenness value (in the descending order) has also been proposed by them (Sun et al. 2021).

It is noteworthy that, apart from criticality-driven strategies, *e.g.*, the betweenness-based one, it will also be equally effective to fulfil the optimization goal (*i.e.*, GWL), through the minimization of T_f in Eq. (4). Accordingly, an accessibility-based strategy, which prioritize the most "accessible" bridge, at each of the decision-moment, has been proposed in this study. Mathematically, such a bridge is set to be one leading to the minimum number of damaged bridges associated with the shortest path between itself and the last bridge partially repaired, at that particular decision-moment.

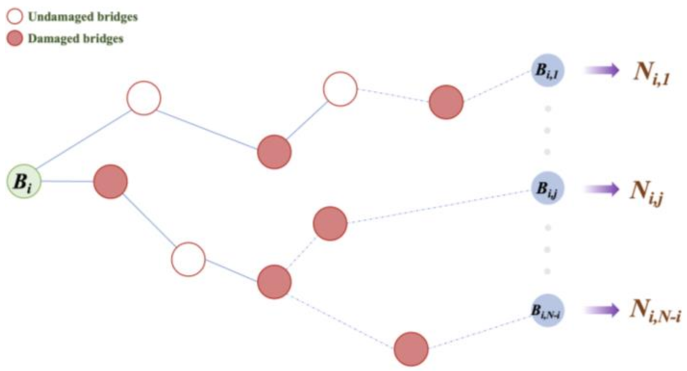

Figure 2. The illustration on the accessibility-based strategy.

For example, Fig. 2 illustrates the decision-moment (would be a total of N ones, in the case of N collapsed bridges. Meanwhile, the first one is the very beginning of the ER campaign) when the i^{th} bridge ($i = 1,2,\ldots,N$) has been partially repaired. Accordingly, with respect to each of the individual collapsed bridge $B_{i,j}$, among the remaining (N-i) ones, $N_{i,j}$ refers to the total number of damaged bridges (with either DS2 or DS3) associated with the shortest path between B_i and $B_{i,j}$. The particular bridge will be therefore picked following Eq. (6), as the p^{th} one:

$$p = arg\,\min_j(N_{i,j}(B_i, B_{i,j}))\ \ (j=1, 2, ..., N\text{-}i) \tag{6}$$

It shall be particularly highlighted that, although this newly proposed strategy aims at minimizing the time span of ER campaigns, it has also taken the criticality of individual bridges into account. Overall, at each of the decision-moment, the more accessible one bridge is, the more critical it also tends to be. On the other hand, such a bridge is more likely to be irrelevant (regarding the connectivity of the whole RN), if hard to reach (*i.e.*, substantial quantity of damaged bridges associated with the short path to it).

3 Case study

3.1 Configuration of the case-study RN

In this research, the MABM, where the ER agent follows the aforementioned heuristics has been applied to the RN across the Luchon Valley, France, as the case-study. As shown in Fig. 3, such a hierarchical RN consists of a *route nationale* (*N125*), several *route départementales*, and rural roads. Given the mountainous topography and considerable amount of water courses, this RN comprises a total of 118 bridges, and connects 53 municipalities (small villages and towns).

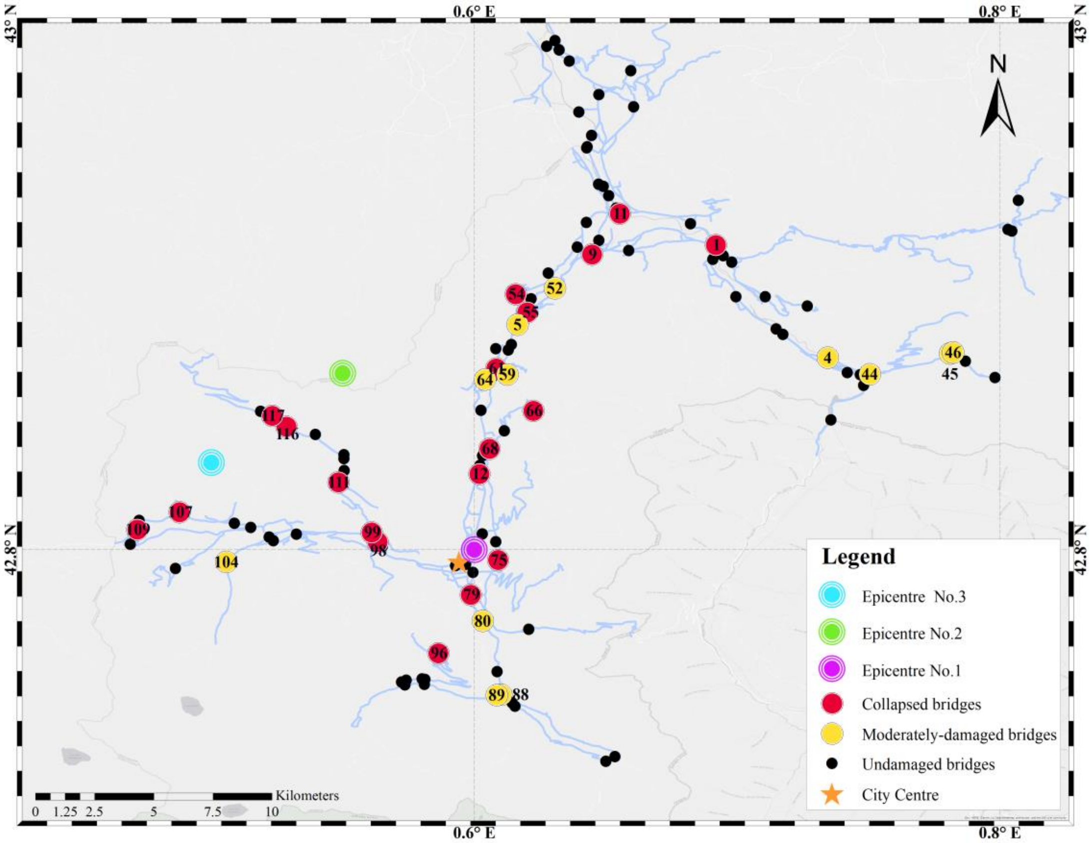

Figure 3. The topology of the case-study RN.

3.2. Scenario-based simulation following the developed ABM framework

Given the significant uncertainties with respect to earthquake hazards, the seismic fragility of the bridges, and the behaviour of the two agents, Monte Carlo (MC) simulations are run to gauge their collective influence on seismic resilience of the whole RN. Specifically, each simulation outcome presented hereinafter is obtained from a total of 2,000 MC runs. Regarding each single realization, the MC simulation starts with the generation of the earthquake scenario, characterized by the location of its epicentre and the seismic magnitude M_w. Based on the recorded historic seismic activity across the region, three epicentres close to the central area of Luchon, with the coordinates presented in Table 1, are considered in this case-study. As shown in Fig. 3, overall, the severity of the damage expected to be triggered by those three epicentres would decrease monotonically, given their closeness to the central area of the city and the whole RN.

Table 1. Location of epicentres.

Epicentre	Longitude (*W*)	Latitude (*N*)
1	0.6	42.8
2	0.55	42.867
3	0.5	42.833

Different ground motion models have been considered as recommended by García-Fernández et al. (2019), and ultimately, the attenuation model associated with a rock site (proposed by Campbell and Bozorgnia in 2008, and is applicable to earthquake scenarios with $M_w \leq 7.5$) has been adopted in this paper. Given the upper limit of the SHARE seismic source area model across the region (Woessner et al. 2013), the maximum seismic magnitude considered in this case-study is set to be 7.

For each individual bridge, its DS will be determined through fragility analysis, based on the intensity measure of the ground motion at its geographic site, obtained from that attenuation model. Besides, the seismic fragility model proposed by Shinozuka et al. (2002) is applied to beam bridges, while the model developed by Zampieri (2014) is employed to investigate the response of arch bridges (Sun et al. 2022).

Table 2. Behavioural attributes of the agents.

Agent	Attribute	Lower	Upper	Distribution	Average repair time
a	V_{er} (km/h)	15	20	Uniform	
	E_{er} (%)	50	100	Uniform	1.5 days
b	V_{fr} (km/h)	5	10	Uniform	
	E_{fr} (%)	5	10	Uniform	15 days

Based on the DS of each individual bridge, the trajectory of the post-shock functionality of the whole RN, driven by the activity of those two Agents described above, will be tracked since the beginning of IAoEs. To that end, in each of the simulation, the behavioural attributes of those agents will be randomly generated following the probabilistic distributions, characterized by the pre-defined parameters. As shown in Table 2, for *Agent a,* the travel velocity (V_{er}) is set to follow a uniform distribution with the lower and upper limits of 15km/h and 20km/h, respectively. Such a relatively low speed is assumed, to consider the potential influence of the debris and jam, throughout IAoEs. In parallel, regarding *Agent b*, who is in charge of the full repair and may thereby need to ship some heavier equipment, the lower and upper limit of its travel velocity, denoted as V_{fr}, are set to be 5km/h and 10km/h, respectively.

In terms of the repair efficiency, for *Agent a*, E_{er} follows a uniform distribution with the lower and upper limit of 100/day and 200/day, respectively. Therefore, the time needed to complete the ER of every individual bridge will range from 0.5 to 1 day. However, it is noteworthy that, this parameter will be reduced by a factor ω^n (ω<1), pursuant to the system-level damage status of the whole RN, at each decision-moment (Eqs. (1-3)). In this paper, the value of ω is set as 0.5, regarding all the simulation outcomes. Furthermore, such a repair time will also increase quadratically with span of the bridge, if larger than 50 m (Eqs. (1-3)). Similarly, the efficiency parameter of (denoted as E_{fr}) of Agent b is also assumed to be following uniform distribution, with the corresponding lower and upper bounds presented in Table 2.

4 Simulation outcome

In this study, median behaviour of the concurrent ER and full repair campaigns will be tracked at first, to model the time-varying resilience behaviour of the RN under any given seismic scenario. Particularly, the impact of different strategies of the ER campaign that have been highlighted above on the seismic resilience of the RN will be gauged. In parallel, the Agent b is assumed to be sticking to the between-based strategy in this study, regardless of the strategy adopted by its counterpart. Besides, in light of the significant uncertainty associated with the earthquake-initiated damage and successive ER campaigns, it will also be strategically vital to assess the resilience behaviour of those physical networks, in "extreme" cases (*e.g.*, the initial damage is exceptionally severe, while the repair efficiency of the two Agents is very low). To that end, 75%- and 95%-quantile of the GWL of the ER campaign associated with each of those strategies will also be considered, in this paper. Furthermore, only the scenario with the magnitude of 7 will be considered in this case-study, to avoid trivial simulation outcomes.

In Fig. 4, the median quantity of bridges with DS2 and DS3 under the seismic scenario with the epicentre No. 1 have both been tracked. It can be found that the median quantity of those two different groups of bridges under such a scenario is 19 and 12, respectively. Accordingly, a representative system-level damage status immediately following the shock under this scenario has been illustrated in Fig. 3.

Regarding the ER of those collapsed bridges, despiste the same behavioural attributes of both the two Agents, the trajectories associated with those three different heuristics are found to be radically different from each other, as shown in Fig. 4(a). Specifically, in terms of the span-based heuristic, the series of long plateaux highlight that the ER campaign is significantly encumbered by the other damaged bridges, and the completion of the entire campaign has thus taken 128.25 days. Meanwhile, by following a different repair sequence, the betweenness-based heuristic has been able to shortens such a time span to 58.5 days, a reduction of 54.4%.

In particular, when it comes to the accessibility-based strategy that always prioritizes those most accessible bridges, the ER has been outpacing both the other two ones, since the very beginning of the campaign. Ultimately, it only takes a total of 45.25 days to wrap up the ER of all the 19 bridges, leading to a reduction of 64.7% (compared to the span-based strategy).

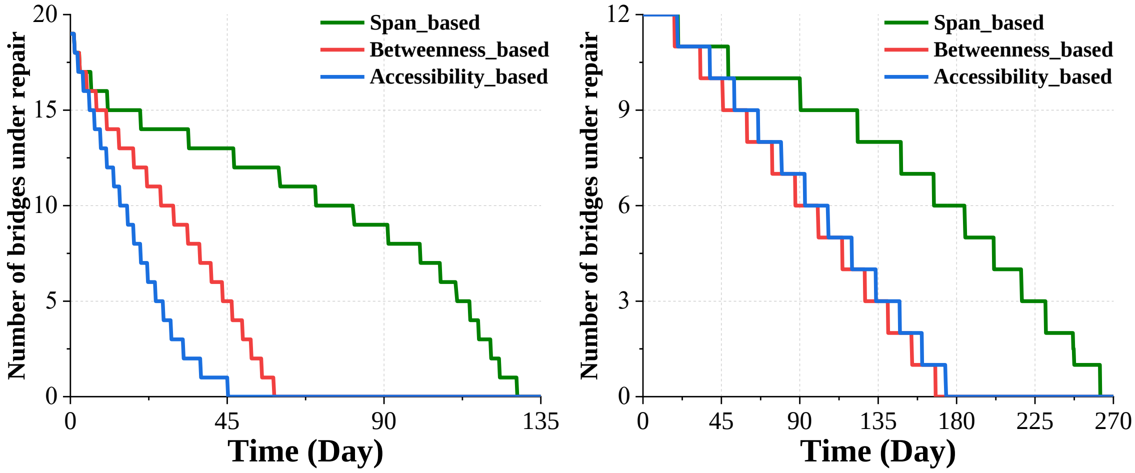

(a) DS3 (b) DS2

Figure 4. Time-varying, median quantity of bridges with different DSs under the scenario with epicentre No.1.

The full repair campaign of those moderately-damaged bridges, run by Agent b, has also been tracked in Fig. 4(b). As mentioned before, irrespective of the strategy adopted by Agent a, Agent b always follows the betweenness-based one, in this study. However, it can be found that the full-repair campaign is also profoundly reshaped by the strategy adopted by *Agent A*, notwithstanding that same strategy of Agent b itself.

In the case of the span-based heuristic, similar to the behaviour of the concurrent ER campaign, the full repair is also revealed to be significantly stalled, due to the bottleneck effect of those not-yet repaired bridges with DS3. Until the 148th day after the shock, when the corresponding ER campaign has already ended (shown in Fig. 4(a)), only 4 bridges have been fully-repaired. It will thus take on average 37 days to do that for each individual bridge, which is much longer than the expected time pursuant to the scope of the parameter of E_{fr} (shown in Table 2). The repair of the remaining bridges has been accelerated thereafter, owing to the removal of the bottleneck of those collapsed bridges. Eventually, all those bridges have been full-repaired on the 262.5th day, since the beginning of the IAoE. This outcome highlights the knock-on effect of the stagnant ER on the full-repair campaign, which will, in turn, further delay the ER campaign itself.

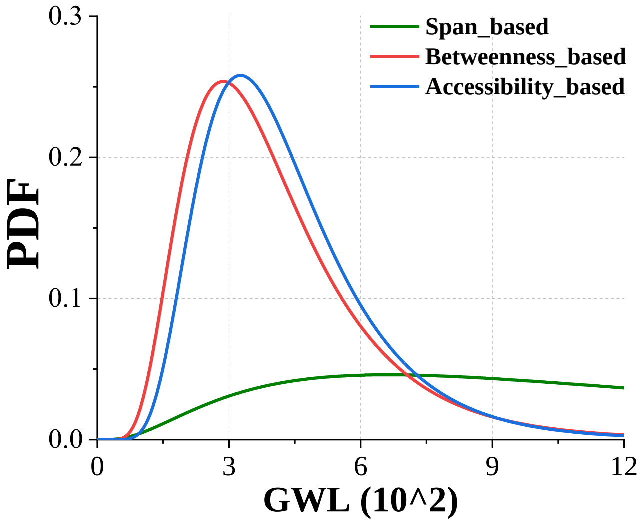

Figure 5. Probabilistic distribution of GWLs under the scenario with epicentre No.1.

Furthermore, it shall be particularly highlighted that, the full-repair campaign has been finalized earlier (168 days versus 174 days), when Agent a adopts the betweenness-based strategy, instead of the accessibility-based one (although not by a huge margin), which is the opposite to the case of the ER campaign. It can be concluded that, despite its rapidity, the accessibility-based strategy has not prioritized the ER of those collapsed bridges that are most relevant to the full-repair campaign. Such an observation has thereby further highlighted the complex interplay between the two Agents, which is also consistent with that with respect to the comparison among the resulting GWLs.

In Fig. 5, following lognormal distribution, probabilistic density functions (PDF) that have been fitted based on the dataset of GWLs generated from the MC runs, with respect to the three different ER heuristics, have all been plotted. In particular, the three quantiles (*i.e.*, the median, 75%-, and 95%-ones, respectively) associated with the fitting and the MC simulation have also been presented and compared in Table 3. Overall, it can be found that the fitted outcomes match the simulated one fairly well, even when it comes to the "extreme" cases. Quantitatively, the discrepancy rate with regard to the 95%-quantile has never exceeded 2%, regarding all the three different heuristics.

Table 3. Resulting GWLs following different heuristics (10^2).

Heuristics	**Span-based**		**Betweenness-based**		**Accessibility-based**	
	Simulation	Fitted	Simulation	Fitted	Simulation	Fitted
Median	14.0055	14.5093	3.6129	3.6343	3.9484	3.9303
75%-quantile	27.6405	26.3780	4.9609	5.0472	5.2785	5.2589
95%-quantile	63.4943	62.3319	8.0398	8.0958	7.8345	7.9954

In both Fig. 5 and Table 3, when it comes to the increasingly more "extreme" cases, the resulting GWL regarding the span-based heuristic has been growing much more sharply, compared to the outcome of the other two ones. Alongside the observation on Fig. 4, it further reveals that the span-based heuristic can potentially trigger substantial socio-economic losses, under catastrophic earthquakes. Meanwhile, it is also noteworthy that, measured by the median, the betweenness-based strategy turns out to be outperforming (compared to the accessibility-based one), notwithstanding the slower ER campaign. However, as highlighted in Fig. 5, the gap between them has been decreasing quick, when it comes to more extreme cases. In particular, the GWL has been reduced by 2.6%, regarding the 95%-quantile, when the accessibility-based strategy has been adopted (Table 3).

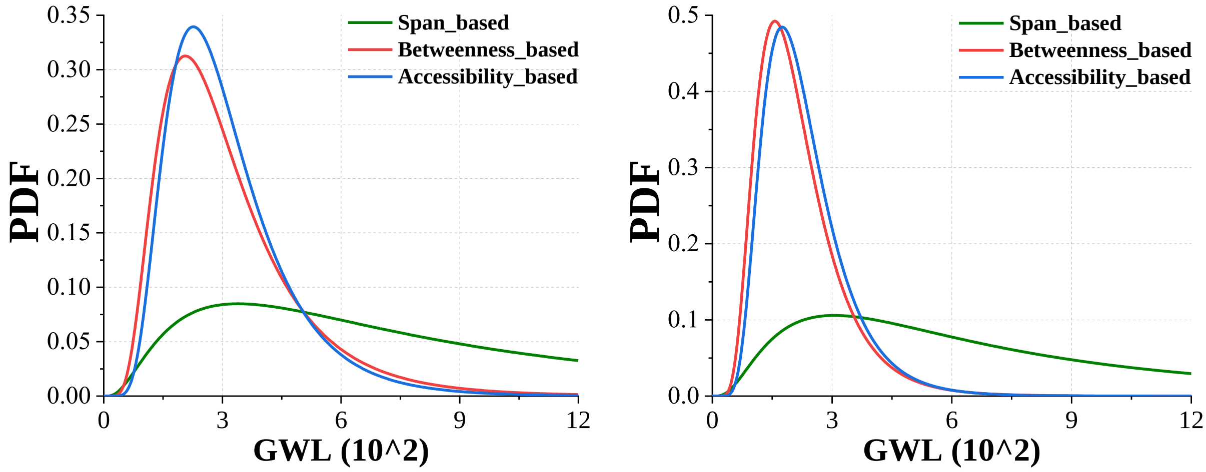

(a) No.2 (b) No.3

Figure 6. Probabilistic distribution of GWLs under scenarios with the other two epicentres.

Such a behaviour, *i.e.*, the accessibility-based strategy is catching up with the betweenness-based one regarding extreme cases has also been observed under scenarios with the other two epicentres. As shown in Fig. 6, in terms of the Epicentre No.2 that is triggering less damage compared to the Epicentre No.1, the median GWL (10^2) associated with the accessibility-based strategy is 3.5% higher than (*i.e.*, 2.7952 versus 2.7016) that regarding the betweenness-based one. However, when it comes to the 95%-quantile, the former strategy has already been able to reduce the GWL, by 9.8%.

Lastly, regarding the Epicentre No. 3 that is inducing the least severe damage, the gap between the GWL associated with the two different strategies has also kept reducing, as far as the more extreme case is concerned. Nevertheless, the accessibility-based strategy has not been able to outperform, measured by the 95%-quantile of GWL (*i.e.*, 4.3051 versus 4.1729), despite the narrowed gap associated with the median measure (following the accessibility-based strategy, the GWL is 2.0859, which is 7.9% higher than 1.9335, regarding the betweenness-based strategy).

In summary, in the case of very widespread and severe damage under catastrophic earthquakes, the accessibility-based strategy can not only accelerate the ER campaign, but also minimize the system-level socio-economic losses.

5 Conclusions

A multi agent-based model (MABM) on post-sock emergency response (ER) of Road Networks (RNs) subjected to catastrophic earthquakes has been proposed. Two agents, who represent the two repair squads running the ER (of collapsed bridges) and the concurrent full-repair campaigns (of moderately-damaged bridges), respectively, have been incorporated into this MABM. In particular, an accessibility-based strategy has been proposed to enable the first agent to plan the ER campaign of RNs, in the wake of damaging earthquakes. To examine its applicability, such a MABM has been employed to model the post-shock ER of a real-world RN in the city of Luchon, France, as a case-study. In particular, another two already-developed heuristics, namely, the span- and betweenness-based ones, have also been included into this MABM, whereby the impact of the different guiding strategy of ER on seismic resilience of the earthquake-impacted RNs can be investigated. To that end, the gross weighted losses (GWL) has been adopted as an inclusive optimization goal of the post-shock ER campaign. Besides, Monte Carlos simulations have been run, to account for the collective impact of the uncertainty of the earthquake ground motion, fragility of bridge structures and the behavioural pattern of the Agents, on the resilience of those RNs. Based on the simulation outcome obtained, it can be concluded that:

1. Given its adaptivity, the developed MABM has enabled a nuanced assessment on seismic resilience of modern RNs;
2. The dynamic and looped interdependence among the ER and the concurrent full-repair campaigns will significantly reshape the resilience behaviour of those physical networks;
3. By prioritizing those most accessible bridges at each of the decision-moment, the newly-proposed, accessibility-based strategy can significantly accelerate the ER campaign. Meanwhile, due to the less importance attached to those most critical bridges, such a strategy is not able to bolster the full-repair campaign, as much as the betweenness-based one does, especially, in the case of limited earthquake-initiated damage;
4. The accessibility-based strategy could, however, reduce the socio-economic losses, when it comes to the extreme case of catastrophic earthquakes.

To conclude, findings in this paper can help to generate new insights, with respect to the planning of emergency response and disaster risk governance of RNs across earthquake-prone regions. However, in view of the interdependence among modern CISs, it will be imperative to come up with a viable approach to the planning of post-shock ER of the interwoven system of CISs. To that end, it will also be strategically crucial to leverage the latest advance in multi-agent deep reinforcement learning, to establish an autonomous decision support system of the real-time and/or near-real-time hazard risk management and mitigation of the integrated community-infrastructure systems imperilled by climate hazards.

6 References

Ausiello, G., Marchetti-Spaccamela, A., Crescenzi, P., Gambosi, G., Protasi, M., and Kann, V. (2003). *Complexity and Approximation (Corrected ed.)*. Springer.

Bashan, A., Berezin, Y., Buldyrev, S. V., and Havlin, S. (2013). The extreme vulnerability of interdependent spatially embedded networks. *Nature Physics* 9(10): 667-672.

Bocchini, P., and Frangopol, D. M. (2012). Restoration of bridge networks after an earthquake: multicriteria intervention optimization. *Earthquake Spectra* 28 (2): 427-455.

Brandes, U. (2001). A faster algorithm for betweenness centrality. *Journal of Mathematical Sociology* 25(2): 163-177.

Brummitt, C. D., Hines, P. D. H., Dobson, I., Moore, C., and D'Souza, R. M. (2013). Transdisciplinary electric power grid science. Proceedings of the National Academy of Sciences 110(3): 12159.

Buldyrev, S. V., Parshani, R., Paul, G., Stanley, H. E., and Havlin, S. (2010). Catastrophic Cascade of Failures in Interdependent Networks. *Nature* 464(7291): 1025-1028.

Campbell, K. W., & Bozorgnia, Y. (2008). NGA ground motion model for the geometric mean horizontal component of PGA, PGV, PGD and 5% damped linear elastic response spectra for periods ranging from 0.01 to 10 s. *Earthquake Spectra* 24 (1): 139-171.

Funabashi, Y., and Kitazawa, K. (2012). Fukushima in review: A complex disaster, a disastrous response. *Bulletin of the Atomic Scientists* 68(2): 9-21.

García-Fernández, M., Gehl, P., Jiménez, M. J., and D'Ayala, D. (2019). Modelling Pan-European ground motions for seismic hazard applications. *Bulletin of Earthquake Eng*ineering 17(6): 2821-2840.

Gehl, P., and D'Ayala, D. (2016). Development of Bayesian networks for the multi-hazard fragility assessment of bridge systems. *Structural Safety* 60: 37-46.

Gehl, P., and D'Ayala, D. (2018). System loss assessment of bridge networks accounting for multi-hazard interactions. *Structure and Infrastructure Engineering* 14 (10): 1355-1371.

Helbing, D. (2013). Globally networked risks and how to respond. *Nature* 497(7447): 51-59.

Kilanitis, I., and Sextos, A. (2019). Impact of earthquake-induced bridge damage and time evolving traffic demand on the road network resilience. *Journal of Traffic and Transportation Engineering (English Edition)* 6(1): 35-48.

Kröger, W., and Zio, E. (2011*). Vulnerable Systems*. London: Springer.

Lin, C. C. J., Hung, H. H., Liu, K. Y., and Chai, J. F. (2010). Reconnaissance observation on bridge damage caused by the 2008 Wenchuan (China) earthquake. *Earthquake spectra* 26(4): 1057-1083.

Mackie, K. R., and Stojadinovic, B. (2006). Post-earthquake functionality of highway overpass bridges. *Earthquake Engineering & Structural Dynamics* 35(1): 77-93.

Nichols, J. M., and Rodgers, S. (2017). Economic and societal challenges imposed by seismic risk on the built environment. *ASCE-ASME Journal of Risk and Uncertainty in Engineering Systems, Part A-Civil Engineering* 3(4): 04017022.

Ouyang, M., Dueñas-Osorio, L., and Min, X. (2012). A three-stage resilience analysis framework for urban infrastructure systems. *Structural Safety* 36-37: 23-31.

Powell, W. B. (2019). A unified framework for stochastic optimization. *European Journal of Operational Research* 275(3): 795-821.

Radio New Zealand (2011). https://www.rnz.co.nz/news/canterbury-earthquake/69187/fire-service-struggling-to-cope-with-rescue-effort (accessed on 30/01/2024)

Shinozuka, M., Feng, M. Q., Kim, H. K., Uzawa, T., and Ueda, T. (2003). *Statistical analysis of fragility curves*. Technical report MCEER-03-0002. *http://shinozuka.eng.uci.edu/Pdf/RepFrag.pdf*

Sun, L. (2017). Modeling the seismic resilience of electric power supply systems. Ph.D. Thesis, Department of Civil, Environmental and Geomatic Engineering, Swiss Federal Institute of Technology Zurich (ETH Zurich), Switzerland.

Sun, L., D'Ayala, D., Fayjaloun, R., and Gehl, P. (2021). Agent-based model on resilience-oriented rapid responses of road networks under seismic hazards. *Reliability Engineering and System Safety* 216: 108030.

Sun, L., Shawe-Taylor, J., and D'Ayala, D. (2022). Artificial intelligence-informed planning for the rapid response of hazard-impacted road networks. *Scientific Reports* 12(1): 1-13;

Woessner, J., Danciu, L., Kaestli, P., & Monelli, D. (2013). *D6.6-Database of seismogenic zones, Mmax, earthquake activity rates, ground motion attenuation relations and associated logic trees*. Seismic Hazard Harmonization in Europe (SHARE) Project Deliverable. *http://www.efehr.org/export/sites/efehr/.galleries/dwl_europe2013/D6-6_SHAREopt.pdf_2063069299.pdf*

Yeh, F. Y., Chang, K. C., Sung, Y. C., Hung, H. H., and Chou, C. C. (2015). A novel composite bridge for emergency disaster relief: Concept and verification. *Composite Structures* 127: 199-210.

Young, S., Balluz, L., and Malilay, J. (2004). Natural and technologic hazardous material releases during and after natural disasters: A review. *Science of the Total Environment* 322(1-3): 3-20.

Zampieri, P. (2014). *Simplified seismic vulnerability assessment of masonry arch bridges*. Ph.D. Thesis, University of Trento, Italy.

Zhang, L. L., Liu, X., Li, Y. P., Liu, Y., Liu, Z. P., Lin, J. C., Shen, J., Tang, X. F., Zhang, Y., and Liang, W. N. (2012). Emergency medical rescue efforts after a major earthquake: lessons from the 2008 Wenchuan earthquake. *The Lancet* 379(9818): 853-861.

Zhao, T., and Sun, L. (2021). Seismic resilience assessment of critical infrastructure-community systems considering looped interdependences. *International Journal of Disaster Risk Reduction* 59: 102246.

Zhao, T., Wang, J., and Sun, L. (2023). Crowd dynamic-based model on post-shock mass evacuation and rescue across urban systems subject to catastrophic earthquakes. *International Journal of Disaster Risk Reduction* 93: 103777.